Biased motion and molecular motor properties of bipedal spiders

Laleh Samii,[1,2] Heiner Linke,[3] Martin J. Zuckermann,[1,2] and Nancy R. Forde[1]
[1]*Department of Physics, Simon Fraser University, 8888 University Drive, Burnaby, British Columbia, Canada V5A 1S6*
[2]*IRMACS, Simon Fraser University, 8888 University Drive, Burnaby, British Columbia, Canada V5A 1S6*
[3]*The Nanometer Structure Consortium and Division of Solid State Physics, Lund University, P.O. Box 118, 22100 Lund, Sweden*
(Received 23 September 2009; published 2 February 2010)

Molecular spiders are synthetic molecular motors featuring multiple legs that each can interact with a substrate through binding and cleavage. Experimental studies suggest the motion of the spider in a matrix is biased toward uncleaved substrates and that spider properties such as processivity can be altered by changing the binding strength of the legs to substrate [R. Pei, S. K. Taylor, D. Stefanovic, S. Rudchenko, T. E. Mitchell, and M. N. Stojanovic, J. Am. Chem. Soc. **128**, 12693 (2006)]. We investigate the origin of biased motion and molecular motor properties of bipedal spiders using Monte Carlo simulations. Our simulations combine a realistic chemical kinetic model, hand-over-hand or inchworm modes of stepping, and the use of a one-dimensional track. We find that stronger binding to substrate, cleavage and spider detachment from the track are contributing mechanisms to population bias. We investigate the contributions of stepping mechanism to speed, randomness parameter, processivity, coupling, and efficiency, and comment on how these molecular motor properties can be altered by changing experimentally tunable kinetic parameters.

DOI: 10.1103/PhysRevE.81.021106 PACS number(s): 05.40.−a, 87.16.−b, 82.39.−k, 87.85.−d

I. INTRODUCTION

Molecular motors are nanoscale machines, capable of transducing chemical energy into biased motion. In biology, molecular motors are the principal agents of motility in living cells, where well-studied examples include kinesin I and myosin V [1,2]. These motors each "walk" unidirectionally along cellular tracks by coordinating binding and hydrolysis of adenosine triphosphate (ATP) between their two heads. On average, a single kinesin motor can take >100 8-nm steps per second [3], can work against loads of approximately 7 pN [1,2], and can take >100 steps before detaching from a microtubule [4,5]. These features of speed, efficiency, and processivity are key parameters of motor performance.

Biological motors such as kinesin and myosin V have inspired the design and construction of synthetic bipedal motors. DNA has proved an excellent construction material for such devices due to its ability to follow well established rules of assembly. While initial DNA machines required external interaction to fuel directed motion, more recent designs have incorporated autonomy, through asymmetry of foot binding or release, to create bipedal motors that can step along a track in a biased fashion [6–10]. In most cases, biased stepping arises because of track asymmetry (from its initial design [7,9] and/or by changes induced by motor activity [7–9]), though a recent example demonstrates that it is possible to incorporate asymmetry into design of the motor alone [6]. The energy source for biased stepping has been DNA hybridization [6,7,9] or hydrolysis [8], while the steps themselves have been accomplished via diffusive thermal motion. To date, these DNA-stepping machines have been characterized with bulk techniques, providing insight on motor bias and estimates of processivity [8,9], though only one experimental study has investigated runs extending beyond a few steps, finding processive behavior [8]. Motor parameters such as stall force and efficiency, best determined in single-molecule experiments [1,2], have only been theoretically estimated and just for one of these motors [6]. There is a clear need for understanding how experimentally designable parameters of these motors, such as step size and kinetics of track binding and release, can be tuned to optimize motor performance.

In this work, we use Monte Carlo simulations to gain an understanding of the operational principles of one of these synthetic motile DNA assemblies, the bipedal molecular spider construct of Pei *et al.* [8]. This spider consists of a hub joining two "legs," each of which is a deoxyribozyme capable of binding to, cleaving, and releasing from a specific single-stranded DNA (ssDNA) sequence [Fig. 1(a)]. In the experiments, a large number of spiders was released onto a "carpet" [quasi-two-dimensional (2D) matrix] of substrate ssDNA and the activity of the spiders was inferred from the loss of substrate DNA as monitored by surface-plasmon resonance. The results suggested that the spiders exhibited biased motion, moving preferentially toward uncleaved substrate rather than remaining in an already-cleaved patch of product DNA, and were able to remain bound to the matrix for multiple catalytic turnovers (i.e., were processive). Pei *et al.* also studied the dependence of speed and processivity on tunable experimental parameters, demonstrating, for example, that increasing the binding strength of legs to substrates led to increased spider processivity.

Since the measurements were performed on a large ensemble of spiders and directly probed only their activity (cleavage) rather than their motility, many aspects of their performance as molecular motors remain unaddressed. Previous theoretical one-dimensional (1D) models have examined the role of biased diffusion in spider motility, first by applying a master-equation approach to different stepping mechanisms and number of spider legs [11] and then by using a first-passage-time approach to the non-Markovian problem that considered the role of memory in biased motion (i.e., explicitly considering the leg's action of converting substrate into product, which alters the probability of leg unbinding) [12].

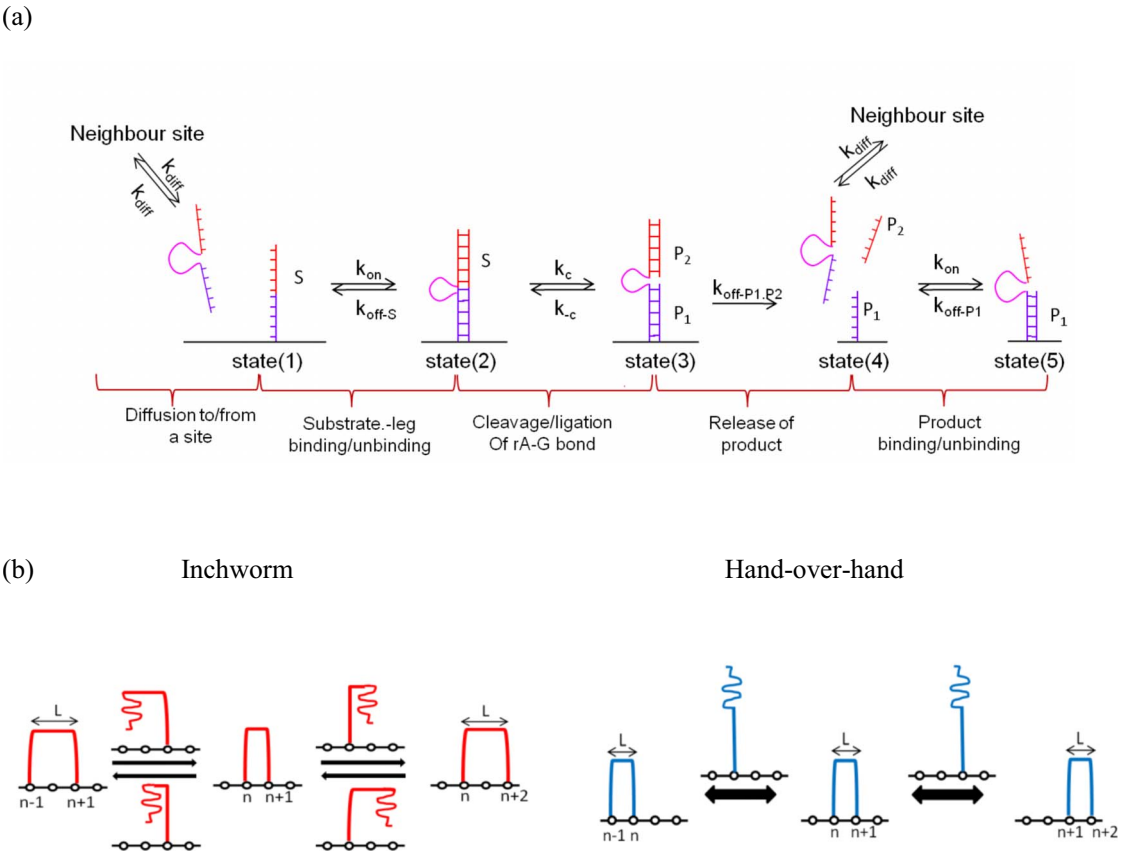

FIG. 1. (Color online) (a) Kinetic model and possible pathways of a leg-track interaction. The values of all rate constants are given in Table I. (b) Stepping mechanisms of IW and HOH spiders.

While providing insight into some of the mechanisms responsible for spider motility, previous theoretical treatments did not consider other aspects of the spider mechanism that may be important for understanding the operational principles of these as motors. For example, detailed kinetics of substrate binding, cleavage, and product release are only implicitly contained in the choice of unbinding probabilities, but since these are values that can be manipulated experimentally [8], a detailed kinetic model of the spider cycle could provide a framework for optimizing desired aspects of motor performance. Also, spiders were treated as infinitely processive, i.e., the models required at least one leg of the spider to be bound at all times. The loss of spiders from the matrix is observed experimentally [8], implying that considerations of processivity are necessary to fully characterize performance. Finally, the ability of the spider to undergo biased motility in the absence of load implies that it should be able to do work against an applied load. For synthetic bipedal walkers to be useful transport devices, this ability to perform useful work is critical, making it important to quantify stall force.

Here, we develop a kinetic model for spider motility that allows us to address questions of how bipedal spiders perform as molecular motors, an approach that should be easily generalizable to other motor systems. While the experiments that stimulated our work examined spiders with two and more legs, here, we limit our study to bipedal spiders to allow investigation of how stepping mechanism impacts motor performance. Our treatment incorporates a kinetic description of binding, substrate cleavage, and dissociation from substrate and product into simulations of the motility and processivity of a bipedal spider. By explicit incorporation of an underlying kinetic scheme for the spider's cycle, our approach allows us to characterize important aspects of the spider mechanism not considered in previous models [11,12]. First, the kinetic cycle gives rise to an imperfect memory effect by allowing dissociation of a leg from substrate to compete with substrate cleavage. Second, the possibility of spiders with finite processivity arises naturally from this kinetic model, since unbinding of a single bound leg competes with rebinding of the second leg.

Stochastic effects arising from competing chemical kinetic pathways are not easily incorporated in an analytical framework, hence, we use Monte Carlo simulations with experimentally derived rate constants to model trajectories of bipedal spiders on 1D tracks. Using these trajectories, we analyze the spiders' performance as motors by characterizing properties such as bias (directionality), speed, randomness parameter, processivity, mechanochemical coupling, and efficiency (via estimation of the stall force). We compare these results for the two simplest mechanisms of bipedal motility, namely, inchworm (IW) and hand-over-hand (HOH), to determine how these two types of stepping mechanism contribute to motor performance. The kinetic model developed here provides insight into the dependence of motor activity on experimentally tunable rate constants, which can be easily

TABLE I. Rate constants of transitions for leg-substrate/product interactions.

Rate constant	Physical meaning	Value (s^{-1})
k_{on}	Substrate binding	20[a,b]
$k_{off,S}$	Substrate unbinding	0.035[a]
k_c	Cleavage	0.055[a,c]
k_{-c}	Religation	0.0005[a,c]
k_r	Release of product	0.046[a]
k_{on}	Product binding	20[a,b]
$k_{off,P}$	Product unbinding	0.14[d]

[a]Estimated from [8,14].
[b]In some of the simulations, k_{on} is changed to 2.4 s^{-1}.
[c]In some of the simulations, k_c is changed to 0.0055 s^{-1} and k_{-c} is kept at $k_c/100$.
[d]Reference [8].

adjusted *in silico* to characterize their effect on motor performance. We demonstrate the feasibility of this approach by determining how motor characteristics change when the rate of binding or cleavage is altered. Our results also shed light on the mechanisms responsible for biased motion of molecular spiders and make predictions of their ability to perform work against an externally applied load.

II. MODELING

A. Kinetic model

In order to study the motion of a bipedal spider, we have established a simple kinetic model for the interaction of a deoxyribozyme leg with its substrate based on previous studies of (deoxy)ribozyme kinetics [13,14]. Figure 1(a) shows the possible kinetic pathways for a leg in its interaction with a substrate and/or product. The possible states of each leg are described as follows. $E+S$ represents an unbound enzymatic leg (E) and a surface-bound substrate (S) (state 1). In ES, the substrate-bound state, an active enzyme-substrate complex forms through base paring of the leg and substrate (state 2). From ES, a leg can either cleave the substrate to form a complex of enzyme and products, EP_1P_2 (state 3), or dissociate to give an unbound leg and a substrate ($E+S$). From EP_1P_2, the complex can either religate to ES (state 2) or proceed with dissociation of the leg from the products, $E+P_1+P_2$ (state 4). Because P_2 diffuses into solution after its release, resulting in a negligible concentration of free P_2 [8], we assume the dissociation of P_2 to be irreversible. After release of the leg from the products, the leg can rebind either to the remaining surface-bound product (EP_1, state 5) or to a new neighbor site, which could be either S (state 2) or P_1 (state 5).

In our simulations, the transition rates between states are specified by the rate constants in Table I. Product binding and unbinding rates k_{on} and $k_{off,P}$ were experimentally determined and k_c is estimated from values provided for the bipedal spider NICK-2.4A [8]. We have assumed a leg to bind at the same rate to a substrate as to a product. We have converted from the measured second-order k_{on} (in M^{-1} s^{-1}) to an effective first-order k_{on} by using an estimated local concentration of a free leg when the second spider leg is bound. The remaining rate constants are estimated based on the kinetic mechanism of the hammerhead HH10 ribozyme [14].

Besides the time scales for biochemical reactions, we must also consider the time scale for diffusion, which enables the spider to explore possible binding sites. By approximating the bipedal NICK-2.4A structure as a sphere of radius 6 nm, we estimated its translational diffusion constant in water. We find that the spider can diffuse over an average distance of 9 nm between adjacent binding sites [8] orders of magnitude faster ($\sim 10^{-6}$ s) than it can bind to substrate (~ 0.05 s). Thus we ignore the time scale of diffusion in our simulations and in the absence of applied force, we assume that a spider leg can bind with equal probability to all allowed binding sites (see below).

B. 1D track

In our model, we replace the "carpet" of ssDNA substrates with a 1D lattice of 1000 sites, which allows for a straightforward assessment of biased motility. The distance between neighboring sites is $\Delta x=1$ unit of length, a dimensionless parameter in the simulations that corresponds to the estimated intersubstrate distance of 9 nm [8].

In this work, we consider three different tracks, denoted P, S, and P-S. The S (P) track represents a lattice of all substrate (product) sites while the P-S track represents a 1D lattice where the left side of the track (sites 1–500) has only product sites and the right half of the track (501–1000) has only substrate sites. The P-S track was chosen for ease of examining bias of spider motion.

C. Stepping mechanisms

We model the spider as two identical physically coupled legs moving on the track. The spider legs are not allowed to occupy the same lattice site, i.e., they interact via exclusion. Here we consider separately two possible mechanisms of spider stepping, IW and HOH [Fig. 1(b)]. For the IW spider, rebinding of a leg is permitted either to its original site (resulting in a center-of-mass change of the spider $\delta=0$) or to its nearest neighbor ($\delta=0.5$ or -0.5). In the HOH spider, rebinding of a leg to its original site is again permitted ($\delta=0$) or it can tumble over the other leg and bind to the next accessible site ($\delta=1$ or -1).

III. COMPUTATIONAL METHOD

A. Kinetics

For a given track, an IW or HOH stepping mechanism, and the chemical kinetic model for each leg (Fig. 1), we performed Monte Carlo simulations of spider trajectories. Each of our simulations started with one spider placed at the middle of a track, such that the initial site coordinates of the legs were taken to be (500, 501). In this situation, the initial biochemical states of the legs are (5, 5), (2, 2), and (5, 2) on P, S, and P-S tracks, respectively (see Fig. 1). The transitions between biochemical states of our kinetic model (Fig. 1) are

Markovian stochastic processes which can be numerically simulated using the Gillespie algorithm [15]. At each step of the calculation, each of the two legs is in one of five biochemical states, with possible kinetic transitions specified by our model. The Gillespie algorithm takes into account all the possible reactions (R_i) from a given state of the system with their specific rate constants (k_i). For example, when the spider legs are in states (5, 2), the first leg can only go to state 4 and the second leg can go to state 1 or 3, giving a total of three possible reactions R_i. By using the Gillespie algorithm, our simulations determine at each step the outcome of this stochastic process: which of these possible reactions occurs and how long it takes. The states of the system and the clock are updated and the Gillespie algorithm is applied to this new state to determine the next transition of the system.

When cleavage of a substrate occurs at a given site, the state of the site is changed from S to P, introducing a memory effect into the dynamics of the spider. In our simulations, we make this site change after the irreversible product release step (rate constant k_r). To explore the role of memory in the bias of the spiders, in some of our simulations we suppress this site change (i.e., the original state of the track is maintained), but otherwise retain the same kinetic scheme.

Our model explicitly includes binding and unbinding of each spider leg to the track, since a leg is unbound from the track when it is in state 1 or 4 [Fig. 1(a)]. If the Gillespie algorithm next selects an unbinding reaction for the other leg, the spider detaches from the track. In most cases, we stop the simulation at this point and consider that the spider has diffused into solution. However, in some of our simulations, we make the spiders infinitely processive by "holding" a detached spider at its last center-of-mass position until a leg rebinds.

In order to analyze trajectories for a large ensemble of spiders, we record 10^6 spider trajectories for each set of parameters tested. For spiders that can detach from the track, a trajectory ends upon detachment. For infinitely processive spiders, however, the trajectory ends when a preset long-time limit is reached. At each kinetic step in all simulations, we record and update the elapsed time, the biochemical state and physical coordinate of each leg, and the state of the track.

B. Application of force

We study the force-velocity relationship for the IW and HOH spiders by applying a force opposing the biased motion of the spiders on the track. In principle, force could act on any of the kinetic steps of binding, cleavage, release, and diffusion [16–18]. However, without knowledge of the force dependence of ribozyme kinetics, we make the simplest assumption that force acts only to bias the choice of binding site by an unbound leg (i.e., it acts on the diffusive, translocation step). Thus, if leg binding is the reaction chosen by the Gillespie algorithm, the choice of binding site is weighted by the force-dependent probability of binding to the forward (+) site over the rearward (−) site

$$\frac{P_+}{P_-} = \exp\left(-\frac{F\delta}{k_B T}\right), \tag{1}$$

where $P_+ + P_- = 1$. Here, F is a rearward force representing a load applied to the spider and δ represents the step size or separation between the center-of-mass positions of the spider in each of the two possible binding sites: $\delta_{\mathrm{HOH}} = 9$ nm and $\delta_{\mathrm{IW}} = 4.5$ nm. Note that here we use real, rather than dimensionless, values for the separations, so that forces are also obtained in real units. In the case of no external force, $P_+/P_- = 1$, i.e., this reduces to equal probability of choosing one of the two allowed binding sites.

C. Calculation of bias and randomness

The ensemble-averaged velocity $\langle v \rangle$ of the spiders is calculated from the slope of $\langle \Delta x_{cm} \rangle$ versus time, where Δx_{cm} is the separation of each spider's center of mass from its starting position of $x_{cm} = 500.5$. The averages are calculated over all spiders remaining bound to their tracks at the specified time. The time window for the average velocity calculation starts at 300 s, a time chosen to be far enough from the initial conditions that transient behavior is excluded, and ends at the latest time at which 1000 trajectories have a spider bound to the track. The time window thus changes for different track, stepping, and kinetic conditions.

In order to quantify the stochastic variability of biased motion, we calculate a dimensionless quantity known as the randomness parameter r given by

$$r = \frac{\mathrm{Var}(x_{cm})}{\langle \Delta x_{cm} \rangle \delta}. \tag{2}$$

Here, δ is the step size of the motor ($\delta_{\mathrm{HOH}} = 1$ and $\delta_{\mathrm{IW}} = 0.5$), and $\langle \Delta x_{cm} \rangle$ represents the drift term, which is given by $\langle \Delta x_{cm} \rangle = vt$. $\mathrm{Var}(x_{cm})$ is the variance of spider positions at time t and is related to an effective diffusion constant by

$$\mathrm{Var}(x_{cm}) = \langle \Delta x_{cm}^2 \rangle - \langle \Delta x_{cm} \rangle^2 = 2D_{eff}t. \tag{3}$$

The randomness parameter has been derived and used in the analysis of motor transport by several authors [3,19–21] and, apart from a factor of 2, its inverse is the Péclet number of hydrodynamics as defined in Ref. [22]. Equation (2) shows that the larger the value of r, the more diffusion predominates over directed stepping.

IV. RESULTS AND DISCUSSION

A. Effect of track properties on biased motion

Sample trajectories of IW and HOH spiders are shown in Fig. 2 in order to provide an illustration of the motion of individual spiders on a P-S track. The directional motion of a population of spiders is studied by ensemble averaging over 10^6 of these trajectories for IW and for HOH spiders. We calculate the probability $P(x_{cm})$ of finding the center of mass of a spider at position x on the track at different times for both IW and HOH spiders. It is important to note that since detachment of spiders from the track can occur, at each time point $P(x_{cm})$ is calculated by averaging only over the spiders remaining bound to the track at that time. Figures 3(a)–3(c) show the evolution of $P(x_{cm})$ with time for HOH spiders on P, S, and P-S tracks.

HOH spiders on a pure P track exhibit symmetric Gaussian probability distributions about the center ($x = 500.5$) of

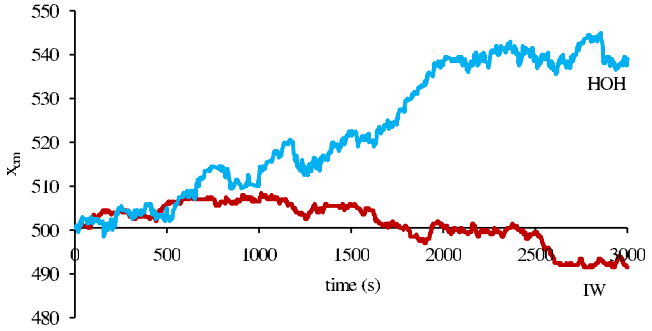

FIG. 2. (Color online) Sample trajectories of an IW spider and of a HOH spider.

the track that broaden as time increases [Fig. 3(a)]. This is a characteristic of unbiased diffusion and confirms that there is no biased motion for the HOH spiders on a pure P track, as one would expect. Similarly diffusive motion was observed for IW spiders on a P track (data not shown).

In contrast to this purely diffusive motion, HOH spiders on an S track clearly exhibit outward bias from the center of the track, as seen in Fig. 3(b). The $P(x_{cm})$ distributions are bimodal due to the lack of initial asymmetry in the system: the initial cleavage happens randomly either with the left or the right leg of each spider. Modification of this (left or right) track site from S to P imposes an asymmetry on the system and spider motion then appears to propagate outward away from this initial cleavage site. Similarly bimodal and outwardly biased probability distributions were observed for IW spiders on an S track (data not shown).

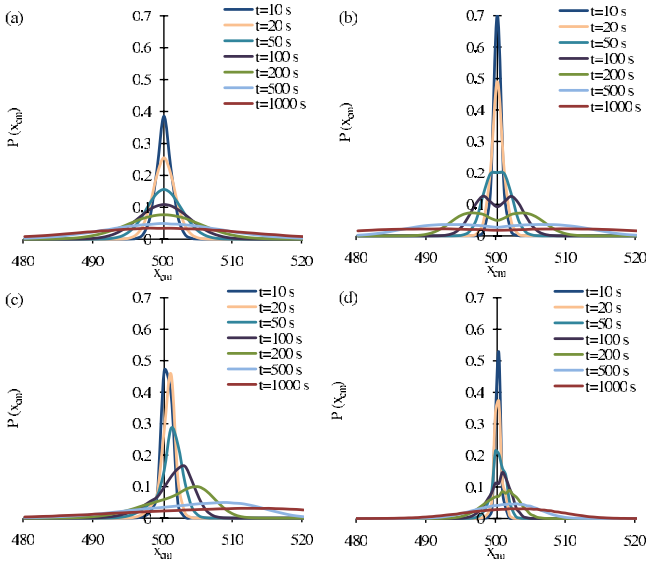

FIG. 3. (Color online) Evolution of position probability distributions $P(x_{cm})$ for HOH spiders on (a) P tracks, (b) S tracks, (c) P-S tracks, and for (d) IW spiders on P-S tracks for the bipedal spider model with both cleavage and detachment. In all cases, the initial number of spider trajectories is 10^6. $P(x_{cm})$ at each subsequent time is calculated only using trajectories that still have a spider bound to the track at that time. For clarity, HOH spider distributions are smoothed by combining probabilities of successive site occupation. This is necessary because the HOH spider spends significantly more time in states where both feet are bound to the track (half-integral x_{cm}) compared to states in which only one foot is bound (integral x_{cm}).

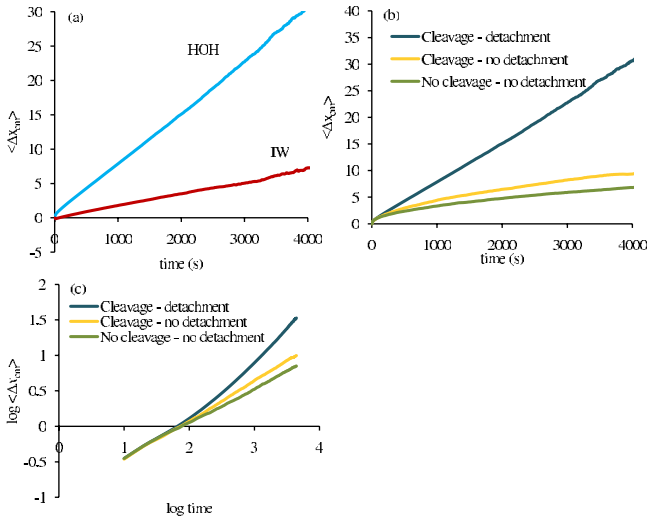

FIG. 4. (Color online) (a) Graph of $\langle \Delta x_{cm} \rangle$ vs time for IW and HOH spiders on P-S tracks. $\langle \Delta x_{cm} \rangle$ is the ensemble-averaged center-of-mass displacement of spiders with respect to their initial position at the middle of the track. It is clear that a population of HOH spiders exhibits much greater speed than IW spiders. (b) Graph of $\langle \Delta x_{cm} \rangle$ vs time for different classes of HOH spiders. Spiders capable of cleavage and detachment show the greatest average displacement vs time. (c) A plot of $\log\langle \Delta x_{cm} \rangle$ vs $\log(t)$ shows that the bias of spiders with neither cleavage nor detachment is diffusive, with a slope of this plot of 0.5. The other two classes of spiders show enhanced biased motion.

The initial symmetry of the track and subsequent symmetry of the P states produced by the population of spiders as a function of time make it challenging to analyze the bias on a purely S track. Thus, we choose to introduce track asymmetry into our simulations to make it easier to observe and quantify the bias of spiders in response to different stepping and kinetic conditions. Evolution of $P(x_{cm})$ on a half-P/half-S (P-S) track (see Sec. II B) clearly exhibits the expected directional motion toward the S side of the track for both HOH spiders [Fig. 3(c)] and for IW spiders [Fig. 3(d)]. We use this P-S track for the rest of our studies as it simplifies analysis of biased motion.

B. Mechanism of biased motion

There are a variety of possible mechanisms that may contribute to biased motion of the population of spiders: system memory effects introduced by modification of the track from S to P, differences in dwell time on S and P sites, and preferential loss of spiders on the P side of the track. In this section, we present and discuss the results of our simulations examining the contributions of these different mechanisms.

In Fig. 4(a), we plot the average displacement of the center of mass $\langle \Delta x_{cm} \rangle$ of IW and HOH spiders as a function of time. In our calculations, Δx_{cm} is defined as the displacement of spider's center of mass from its initial position (x_{cm} =500.5). The plots show that the HOH stepping mechanism leads to an approximately 4 times greater speed than the IW

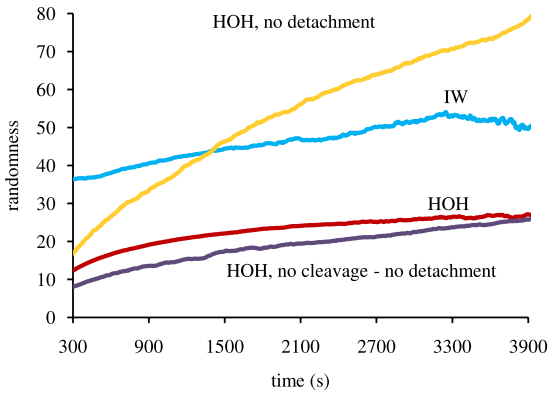

FIG. 5. (Color online) When cleavage and detachment are both permitted, the randomness parameter is greater for IW than HOH spiders. Removing detachment from HOH spiders results in increased values of r, while r reduces substantially when cleavage is also disallowed. In all cases r increases with time.

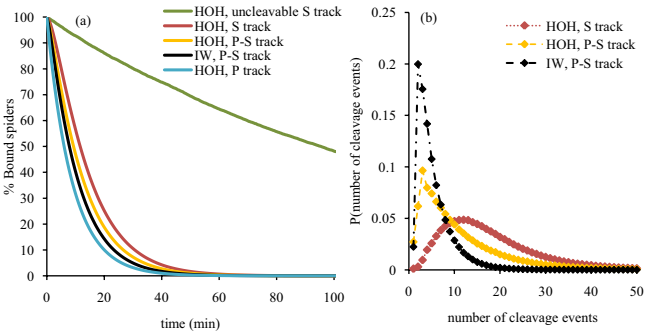

FIG. 6. (Color online) (a) Percentage of trajectories with bound spiders as a function of time, for HOH spiders on S tracks, on P-S tracks, on P tracks, and on uncleavable S tracks, and for IW spiders on P-S tracks. Spiders exhibit the longest dwell times on uncleavable S tracks and detach most rapidly from P tracks. (b) Probability distributions of the number of cleavages performed by each spider prior to its detachment from a track. HOH spiders exhibit greater processivity than IW spiders and their processivity is significantly enhanced on S tracks. Lines through the points are guides to the eyes.

mechanism, as seen in Figs. 3(c) and 3(d). About half of this difference could be ascribed to the factor-of-2 difference in step sizes ($\delta_{\mathrm{IW}}=0.5$ and $\delta_{\mathrm{HOH}}=1$). This would still leave a factor of approximately 2 difference in speed, suggesting that the stepping mechanism has a role in determining the magnitude of bias.

To examine the extent of stochastic broadening of the biased motion of each type of spider, we calculate their randomness parameters r using Eq. (2). We find that r increases with time for both IW and HOH spiders and that r is greater for IW spiders than for HOH spiders (Fig. 5). For IW spiders, both $\langle \Delta x_{cm} \rangle / \mathrm{Var}(x_{cm})$ and step size are smaller than for HOH spiders.

Our kinetic model provides an asymmetry between S and P sites via the average dwell time of a leg on a substrate (25 s) versus product (7 s). The shorter dwell time of a leg on a P versus S site means that it is more probable (per unit time) that a leg dissociate from the P side of the track. Thus, one must consider that part of the observed population bias could be the result of preferential detachment of spiders from the P side of the track (see Fig. 6). To determine the influence of detachment of spiders from the track on the observed biased motion of the bound population, we simulate HOH spiders on a P-S track following the same kinetic scheme as shown in Fig. 1(a) but that are kept from leaving the track by holding a detached spider at its last center-of-mass position until a leg rebinds. We call this case "spiders with cleavage and without detachment." It is important to note that this is a purely artificial construct, designed to probe the role of detachment, and is not achieved in experiments, where spiders have a finite binding time to the substrate matrix.

In Fig. 4(b), we see that the average displacement of HOH spiders decreases when detachment is not permitted. However, disallowing detachment results in a significant increase in r for HOH spiders. This is predominantly due to their decreased speed, since the variance is almost identical for spiders with and without detachment (data not shown). The calculated values of the randomness parameter r for HOH spiders with cleavage and without detachment show that, similar to spiders with cleavage and detachment, r increases with time (Fig. 5). It should also be noted that in this case of cleavage without detachment, r is again smaller for HOH spiders than for IW spiders (data not shown). These results indicate that detachment contributes significantly to the biased motion of the population and, thus, that the observed bias for spiders with cleavage and detachment is in part a result of spiders leaving the track preferentially from the P side.

Previous theoretical treatment has assumed track cleavage to play a major role in promoting biased motion [12]. In these models of the spider, cleavage of an S to a P site was deterministic, based solely on the binding of a spider leg (i.e., cleavage was 100% efficient). In such a case, the movement of the P-S boundary could be used as an indicator of spider population speed. In our kinetic model, by contrast, binding of a leg to an S site is not necessarily followed by cleavage: detachment without cleavage is allowed. This makes it less obvious how strongly track cleavage contributes to the population bias.

We address the question of how much track cleavage (i.e., non-Markovian or memory effects) contributes to the observed bias of the spider population by examining HOH spiders that can neither cleave nor detach. Here, the spiders again follow the kinetic scheme shown in Fig. 1(a) but they are not allowed to detach from or cleave substrates on the track. Therefore, the state of the track is not changed from substrate to product when a transition from state 3 to state 4 occurs and spiders are forced to stay on the track, as above. It is worth noting that for both of these artificial spider models, with cleavage and without detachment and with neither cleavage nor detachment, it is important to keep the same kinetic scheme as the original spiders so as not to change the time scale of the leg-track interaction.

Shown in Fig. 4(b) is a graph of $\langle \Delta x_{cm} \rangle$ versus t for the HOH spiders with neither cleavage nor detachment, demonstrating that the bias is further reduced but is still present when both cleavage and detachment are removed. These re-

sults support the hypothesis that track cleavage (spider "memory") improves the directionality of spider motion. It is, however, surprising that a population of spiders undergoing only effective diffusion on asymmetric tracks is capable of biased motion. What could be responsible for this? A third possible factor contributing to bias is the free-energy preference for binding to S versus P, manifest in our kinetic simulations by the leg dwell times on S and P sites. This hypothesis suggests that we should observe spiders with neither cleavage nor detachment to preferentially populate the S side of a P-S track. Indeed, our simulations show that the ratio of spiders on S:P sides of the tracks increases from an initial value of 1 to a plateau of 6.1 after approximately 300 s. A statistical mechanical calculation, using partition functions to describe states with free energies of a bipedal spider binding zero, one or two legs to the S side versus the P side of the track, predicts a much larger ratio of 15. Clearly, this statistical argument, based on thermodynamics, overestimates the preference for S-site occupation compared to our simulations. It is, however, important to note that our artificially constrained spiders "without detachment" sample a reduced phase space compared to experimentally realizable spiders and hence may not be able to perform a proper sampling of states required by this Boltzmann treatment. Alternatively, we can consider the contributions of effective diffusion, where the populations on P tracks or on uncleavable S tracks evolve with $D_P > D_S$ due to the shorter dwell times on P sites (data not shown). A heuristic argument can be made that a free-energy bias toward S-state occupation is counteracted by an effective diffusional drift toward the P side of the track. Such a population drift toward the P side is predicted in some treatments of state-dependent diffusion [23,24], which calculate $\langle \Delta x_{cm} \rangle$ to evolve with $\sqrt{t}$ toward the region of greater diffusion constant. Our simulations result in $\langle \Delta x_{cm} \rangle \propto \sqrt{t}$, but with a bias to the S side of the track, the region of *lower* effective diffusion constant [Fig. 4(c)]. The biased motion of this artificial model system of bipedal spiders with neither cleavage nor detachment is somewhat surprising, illustrating the ability of the Gillespie-based Monte Carlo approach to uncover dynamics that may not be apparent from separate treatments of thermodynamics and diffusion.

Like the other classes of spider, spiders with neither cleavage nor detachment exhibit an increasing randomness with time (Fig. 5). However, the removal of cleavage from spiders unable to detach results in a drastically reduced r. It is surprising that the least "random" of our spiders are these that have no memory effect and are capable only of effective diffusive motion. Although the velocity is lower for these spiders than others, their substantially reduced variance results in their smaller value of r by Eq. (2) (data not shown). This is likely a result of increased population on the permanently S side of the track (see above), where diffusion is much smaller than on P sites.

In the remainder of this work, we describe the molecular motor properties of the bipedal spiders capable of both cleavage and detachment, since this is the most realistic of the models considered here.

C. Processivity

Next, we investigate the influence of the stepping mechanism on processivity for both IW and HOH spiders. By definition, processivity of a motor is the number of catalytic cycles (cleavage events) before detachment from its track. High processivity is one of the desired features when designing a molecular motor.

By analogy with experiment [8], we first calculate the percentage of spiders remaining bound to their respective tracks as a function of time [Fig. 6(a)]. These results show most rapid detachment from a P track and slowest detachment from an uncleavable S track (in agreement with experiments) and faster loss of IW than HOH spiders. To simulate an uncleavable S track [8], we allowed only transitions between states 1 and 2 (Fig. 1). In almost all cases studied, the vast majority of spiders detach by 30 min.

We investigate processivity by calculating the probability distributions of the number of cleavage events for IW and HOH spiders before detachment from the track [Fig. 6(b)]. These results show HOH spiders to be more processive than IW spiders. The longer binding time and increased processivity of HOH compared to IW spiders can be rationalized by analyzing their respective stepping mechanisms. Consider the initial configuration of a spider at sites (500,501) bound to states (P,S). Due to the shorter dwell time, a leg bound to the P site is more likely to unbind than a leg bound to the S site. In the case of the IW spider, the available binding sites for the mobile leg are the nearest (500) and next-nearest neighbors (499) of the bound leg, i.e., both on the P side of the track. However, in the case of the HOH spider, the reachable binding sites are the nearest neighbors of the bound leg, in this case a P site (500) and an S site (502). The HOH spider, therefore, has an earlier opportunity to bind to a new S site, which increases its binding time to the track. Additionally, the increased accessibility of S sites to the HOH spiders increases the possibility of a cleavage event.

In agreement with the proposed role of binding to S in enhancing processivity, we find that HOH spiders perform significantly more cleavage events prior to detachment when they are initially bound in the center of an all-S track [Fig. 6(b)]. The much increased processivity in this case is the behavior that would be expected of the experimental spiders, sparsely distributed within a substrate matrix [8].

D. Mechanochemical coupling

Another key parameter of molecular motors is mechanochemical coupling, which indicates the correlation between mechanical steps and chemical cycles. In order to characterize the mechanochemical coupling of IW and HOH spiders, we have calculated the spatial correlation of sequential cleavages (Fig. 7). This calculation shows that 81% of IW spiders will sequentially cleave adjacent S sites ($\Delta x = +1$), while only 34% of HOH spiders exhibit sequential cleavage of neighboring S sites in the direction of population bias. Thus, the data show a tight coupling between mechanical and chemical cycles of IW spiders but a weaker coupling for HOH spiders. From the same figure, it is clear that there is also a considerable probability of HOH spiders cleaving the rearward neighbor ($\Delta x = -1$) and next-nearest forward neighbor ($\Delta x = +2$), while these probabilities are very small for IW spiders. We conclude that the ability of HOH spiders

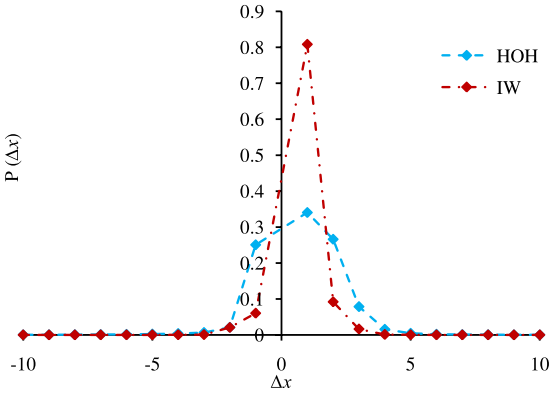

FIG. 7. (Color online) Probability distributions of separation between sequential cleavage events for IW and HOH spiders on *P*-*S* tracks, showing tighter mechanochemical coupling for IW spiders. Lines through the points are guides to the eyes.

to "tumble" along the track provides easier access to further sites, which while increasing their speed, reduces their mechanochemical coupling.

Having tightly coupled mechanochemistry serves two important roles in the function of spiders as molecular motors. First, tighter coupling between cleavage and motion results in more efficient use of the fuel for stepping, with fewer unproductive cleavage cycles that do not couple to motion. Importantly, tighter coupling also means that bound substrates are more likely to be cleaved, which in turn reduces the likelihood that patches of uncleaved substrate could remain behind the spider to act as backward "traps" to the desired forward bias. This relationship between cleavage probability and mechanochemical coupling is further illustrated by the reduced coupling found when the cleavage rate is lowered by an order of magnitude in our simulations. (Experimentally, this could be achieved by lowering the concentration of Zn^{2+}, a necessary cofactor for cleavage.) In this case of $k_c=0.0055\ s^{-1}$, we find from our simulations that the percentage of spiders that sequentially cleave adjacent sites is reduced to 38% and 21% for IW and HOH spiders, respectively. This example illustrates the role that individual, experimentally tunable rate constants play in optimizing specific aspects of motor performance.

E. External force

Both to gauge the spiders' performance relative to their biological counterparts and to evaluate their possible work output as synthetic motors, we investigate the force-velocity relationship and determine the stall force (the force at which the average velocity drops to zero) for both IW and HOH spiders. To do this, we incorporate the typical intersubstrate distance of experiments, $\Delta x=9$ nm, to determine velocity and force [using Eq. (1)]. For each applied force used in our simulations, we calculate the spiders' average velocity from the slope of $\langle \Delta x_{cm} \rangle$ versus t. The resultant plots of velocity versus force for IW and HOH spiders are shown in Fig. 8(a). For both types of spider, the velocity decreases in response to applied force before reaching stall conditions at approximately 0.045 pN for both IW and HOH. For forces greater than the stall force, the spiders preferentially walk backward toward the *P* side of the track.

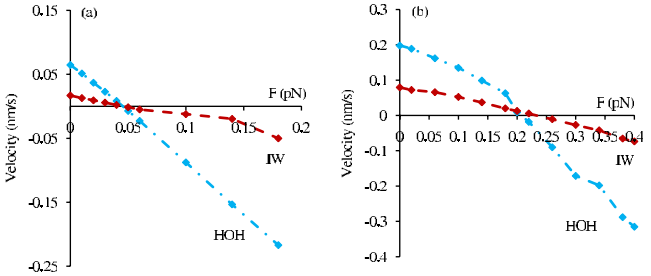

FIG. 8. (Color online) Graphs of velocity vs force for IW and HOH spiders on *P*-*S* tracks with (a) $k_{on}=20\ s^{-1}$ and (b) $k_{on}=2.4\ s^{-1}$. Decreasing the binding rate increases the stall forces, which are very similar for HOH and IW spiders. Lines through the points are guides to the eyes.

Figure 8 shows that the slope of v versus F for HOH spiders is greater than for IW spiders. This is consistent with the effect of a given load to increase the rearward bias for HOH spiders ($\delta_{HOH}=9$ nm) compared to IW spiders ($\delta_{IW}=4.5$ nm) [see Eq. (1)]. However, the velocity of HOH spiders at $F=0$ is larger than for IW spiders. Hence it is reasonable to expect that the graphs of v versus F for IW and HOH spiders should intersect as observed in Fig. 8. Where these curves intersect, however, as well as which stepping mechanism should give a larger stall force, depends on the specific biochemical kinetics and cannot be derived analytically; rather these types of issues can be addressed only through simulations such as the ones reported above.

These values of the stall force are much lower than for biological motors such as kinesin. The stall force of the spider can be increased, as seen in Fig. 8(b) for simulations in which we have decreased the effective binding rate by an order of magnitude, from $k_{on}=20\ s^{-1}$ to $k_{on}=2.4\ s^{-1}$. The larger stall force may be due predominantly to the increased speed at zero force for $k_{on}=2.4\ s^{-1}$, which arises from enhanced detachment of spiders from the *P* side relative to the faster rebinding rate $k_{on}=20\ s^{-1}$ simulations (data not shown).

The thermodynamic efficiency of these spiders can be estimated from the free-energy bias of the reaction and the determined stall force. We first consider the case where substrate cleavage provides the free energy to bias motility. As a value for the free-energy change, we take that of phosphate bond hydrolysis of ATP under standard conditions, $\Delta G^\circ = -30$ kJ/mol. Because of the very low local concentration of P_2 in experiments, the Gibbs free-energy change of $S \rightarrow P_1 + P_2$ will be much lower than ΔG°. In fact, in the limit of $[P_2] \rightarrow 0$ (our simulations), the reaction is irreversible and no free-energy change can be defined. For the sake of argument, we consider $K_{eq}=1$, for which the thermodynamic efficiency is $\eta_{th}=F_{stall}\delta/|\Delta G^\circ|$. Here, F_{stall} is the stall force determined for each motor (Fig. 8) with a step size of δ. For the HOH spider, this gives $\eta_{th,HOH}=0.08$ while for the IW spider, $\eta_{th,IW}=0.04$. It is clear that the spider does not efficiently convert free energy released from substrate cleavage into useful work.

Alternatively, we consider the bias for spider motility to arise from the free-energy preference to bind S versus P and we then determine the force required to remove this bias. This treatment follows similar reasoning used in Ref. [6], although in our kinetic model, a leg binds to S and to P sites at the same rate, while dissociating more rapidly from a P site. To determine the free-energy difference between binding to S and to P (i.e., between states 2 and 5 in Fig. 1), we use the second-order binding rate constant k_{on} [8] and the first-order unbinding rate constants $k_{off,S}$ and $k_{off,P}$ (Table I) to calculate K_{eq} for leg binding to S and to P, from which $\Delta G_{P\text{-}S}$ can be calculated. This results in a free-energy preference for a leg to bind a forward S site over a rearward P site of $|\Delta G_{P\text{-}S}|=3.5$ kJ/mol. The elimination of this energetic preference for leg binding requires the application of a force against this bias: $F_{stall,P\text{-}S}=|\Delta G_{P\text{-}S}|/\delta$. For the two types of stepping mechanism considered here, this argument suggests $F_{stall,P\text{-}S,\mathrm{HOH}}=0.6$ pN ($\eta_{P\text{-}S,\mathrm{HOH}}=0.17$) and $F_{stall,P\text{-}S,\mathrm{IW}}=1.2$ pN ($\eta_{P\text{-}S,\mathrm{IW}}=0.12$). Both this treatment and the one presented in the previous paragraph suggest that the HOH spider is more efficient than the IW spider; again, it is clear that the spider is not efficient at transducing an energetic bias into mechanical work. It is important to note that the efficiencies of a molecular motor and its mechanochemical coupling are independent parameters and are not necessarily related [1], so although the IW spider has high coupling (Fig. 7), it is not necessary that this correlate with a high efficiency.

Consideration of the possible leg configurations shows how the above calculations place only upper limits on the stall force for the spider. The calculations assume that an unbound leg has the choice between binding a forward S site or a rearward P site. If S-site cleavage correlated 100% with leg binding, an assumption made in a previous theoretical treatment [12], the track would retain a distinct boundary between P sites and S sites that would move progressively forward with time and whose movement would relate to spider speed. Our kinetic model, by contrast, allows for leg dissociation from an S site without cleavage (transition represented by $k_{off,S}$ in Fig. 1), making it possible for the spider to step forward without cleaving S from the initially imposed P-S boundary, to have its legs bound later to (S,S) sites and, upon further cleavage, leave an "island" of S sites behind it. Thus, choices of binding possibilities for a leg are not only between a rearward P and forward S (P,S) as considered in the previous paragraph, but also (S,P) (S,S), and even (P,P) for spiders that have stepped diffusively into the product zone. The symmetric binding choices (S,S) and (P,P) are stalled at zero force, while the choice of (S,P) sites generates reverse bias even in the absence of load. The treatment of the previous paragraph, which considered stalling the spider from a (P,S) choice, thus provides an upper limit to the maximum stall force possible for our kinetic model.

It is surprising to observe that HOH and IW spiders exhibit roughly the same stall force, in spite of their different step sizes. HOH versus IW behavior has previously been theoretically investigated for a different model system and, there, HOH and IW stepping gave rise to the same stall force [25]. However, the model assumed the same binding site separation for both types of motion, whereas here, the difference in step size would lead one naïvely to expect that the stall force for HOH should be a factor of 2 lower than for IW. Why is this not the case? If we consider the idealized case of a spider always located at a P-S boundary, we see that detachment of the trailing foot from a P site is more probable than detachment from an S site. For an HOH spider, rebinding of this foot is forward-biased [choice of (P,S) binding sites], while for an IW spider, rebinding of this foot is not biased in either direction [choice of (P,P) binding sites]. In this idealized scenario, therefore, force must work against the forward bias of both feet of an HOH spider, while it needs to work only against the forward bias of the leading foot of an IW spider. This provides a possible rationale for the surprising observation of equal stall forces for both stepping mechanisms in our work.

V. SUMMARY AND CONCLUDING REMARKS

In this study, we presented a kinetic model to investigate the biased motion of a population of bipedal spiders. Using realistic experimental rate constants, we determined that spider bias arises from three contributing factors: (1) preferential occupation of substrates compared to products due to the free-energy difference in leg binding, (2) faster dissociation from products, enhancing the ratio of legs bound to substrate versus to product, and (3) cleavage of substrate, which converts substrate to the weaker leg-binding product.

Our investigations of speed, processivity, mechanochemical coupling, and stall force (efficiency) revealed that bipedal spiders act as molecular motors, albeit only weakly. These characteristics were studied for a large population of spiders and it is clear from trajectories of single spiders that each individual may not exhibit directed motion and hence would not be useful as a molecular motor. Thus, single-molecule studies of spiders would require averaging over many observed trajectories to ascertain their performance and slight directional bias.

We studied two distinct stepping mechanisms in order to better understand their individual contributions to motor performance. Comparing two stepping mechanisms, we find that the increased accessibility to new substrate sites for HOH spiders appears to be responsible for their greater speed and processivity, while the greater coupling and efficiency found for IW spiders suggest they may use the trailing leg as a clamp to maintain the spider in better register with the P-S boundary when compared to HOH spiders that can "tumble" promiscuously past this boundary.

Our calculations for the randomness parameter r of spiders on a P-S track show that in all cases, r is considerably larger than 1, implying that the spider motor is more diffusive than directional. In addition, r increases as a function of time mostly due to the result that the gradient of $\langle \Delta x_{cm} \rangle$ decreases as a function of time, though in some cases, the increase is not very significant. Furthermore, the value of r was found to be higher for IW spiders than for HOH spiders by a factor of 2–3, a factor similar to their difference in step

size. In contrast, previous studies of these two types of stepping mechanism found a value of r close to 1, which was lower for IW motors ($r \sim 0.7$) than for HOH motors ($r \sim 0.85$), indicating a balance between diffusion and directional bias [25]. However, the stepping probabilities that they used strongly forward-biased their motors. It is therefore not surprising that they found values of r which are considerably smaller than our values. It would also be of interest to calculate r as a function of load force for our model [3,25].

The experiments on molecular spiders were performed on an initially symmetric all-substrate surface [8], while we have done most of our simulations on a *P*-*S* track. This initially imposed asymmetry helps to simplify our analysis of biased motion. However, our studies of binding time and processivity have also examined performance on a symmetric *S* track (see Sec. IV C) and clearly show the influence of track construction on these parameters. To extend our model from a 1D track to a quasi-2D matrix is beyond the scope of our current study, but it is certainly feasible using the same Monte Carlo treatment of chemical kinetics for each leg while generalizing the stepping mechanism.

The experimental spider is not limited to an IW or HOH stepping mechanism but is likely to be constrained in leg binding only by the maximum span between legs, L [11]. For $L=1$, only the HOH stepping mechanism is allowed. For $L=2$, motion can consist of IW and HOH stepping, along with larger HOH-type steps that include step sizes of $\delta=2$. Simulations that allow all binding possibilities within the global constraint of $L=2$ show that binding time and processivity increase considerably for these spiders compared to the IW spiders of this study ($L=2$) (data not shown), as would be expected for spiders that are more dominated by HOH stepping. Most remarkably, the calculated speed for these $L=2$ mixed stepping spiders on a 1D *P*-*S* track is $v=0.13$ nm/s (data not shown), almost an order of magnitude higher than we found for IW spiders ($v=0.016$ nm/s). The greater contribution of HOH stepping is likely to be responsible for this increase in speed since for these mixed spiders, we have the possibility of step sizes of $\delta=2$.

In their experimental study of molecular spiders, Pei *et al.* sought to increase processivity in two ways: (1) by increasing the binding strength of legs to substrate and product and (2) by increasing the number of spider legs [8]. They quote few results for the bipedal spider, however, we can see by comparison of detachment rates of two-legged spiders in our model (Fig. 6 for spider on an *S* track) to their reported loss of four- and six-legged spiders from the matrix [Fig. 6(a) in Ref. [8]] that the shape of our spider loss curve is similar to the experimental results and that the time scale of detachment from our model is shorter than reported for four-legged spiders, as expected [8]. Experimental results suggest that adding more legs to the spiders improves processivity but decreases their speed [8]. Preliminary data from our simulations agree with these results: we find that bipedal spiders with a global stepping constraint of $L=3$ travel 3 times faster than quadrupedal spiders with the same constraint, while the processivity of quadrupedal spiders is more than an order of magnitude higher than the bipedal spiders (data not shown). Clearly, altering design elements of synthetic motors can result in significant, and not always commensurate, changes in motor performance. The decrease in speed with increasing number of legs can be contrasted with the transport of particles by multiple kinesins, in which speed was found to be independent of number of motors; in both examples, however, processivity increases with the number of motor units [26].

Our work is related to studies of burnt-bridge motors which serve as theoretical models for the biological motor collagenase [27–29]. Simulations of these motors suggest that, like the molecular spider, they are weak motors with low efficiency. Unlike burnt-bridge motors, the legs of molecular spiders retain the ability to bind to the cleaved products, as seen through our use of $k_{on,P}>0$, and are able to move in either direction from the cleavage site, even if $k_{on,P}=0$. Our spider model is more similar to a model for collagenase that allows the motor to diffuse to either side of a bond following cleavage [30].

Our simulation results demonstrate that the bipedal spider performs far below the standards set by biological motors such as conventional kinesin. Kinesin 1 is well known as a processive molecular motor [31], which *in vitro* can undergo $\sim$150 HOH steps of 8 nm before detaching from a microtubule [4,5]. The processivity of IW and HOH spiders on an all-*S* track is an order of magnitude lower [Fig. 6(b)]. Kinesin furthermore exhibits tight coupling between its mechanical stepping and chemical cycles, such that its velocity is proportional to the rate of hydrolysis with *in vitro* speeds of $v \approx 1$ μm/s [3]. The combination of much faster hydrolysis and efficient coupling of this chemical reaction to forward stepping explains why the speed of kinesin is orders of magnitude greater than HOH and IW spiders, which have roughly the same step size. HOH and IW spiders exhibit weak coupling between cleavage and directional motion and cleavage can frequently be followed by backward steps, particularly for HOH stepping. The spider design lacks mechanical coupling between its legs that could coordinate leg binding and release [32] and has no form of a power stroke to intrinsically bias the motion of a leg in the forward direction [33]. The large randomness parameter found for spiders in our simulations ($r>10$) is further evidence of the dominance of diffusion over biased motion, especially when compared to $r \leq 1.5$ for kinesin [3]. The fuel source for spiders and kinesin is similar, as both hydrolyse a phosphate bond, and their step size is also similar. However, kinesin is capable of working against loads of approximately 7 pN [1], much higher than our predicted stall force of bipedal spiders.

We hope that the approach used here will serve as an experimentally relevant tool to assist in the design of synthetic motors with specific performance measures such as speed, processivity, or efficiency. By using as input experimentally controllable parameters such as rates of binding, cleavage and dissociation, and number of spider legs for the molecular spider, our model creates the opportunity for *in silico* optimization of motor performance.

ACKNOWLEDGMENTS

This research was funded by a research grant from the Human Frontier Science Program. We thank Michael

Plischke for many useful discussions, Eldon Emberly for early guidance with our simulations, and Peter Unrau and Dipankar Sen for assistance with ribozyme kinetics. Thanks to all members of our international motors team and the Forde laboratory for comments on this work and especially to Gerhard Blab and Nathan Kuwada for critically reading the manuscript. Computational resources were provided by Westgrid. N.R.F. acknowledges support from the Research Corporation and the Michael Smith Foundation for Health Research. N.R.F. and M.J.Z. wish to thank NSERC for support.

[1] C. Bustamante, Y. R. Chemla, N. R. Forde, and D. Izhaky, Annu. Rev. Biochem. **73**, 705 (2004).
[2] W. Hwang and M. Lang, Cell Biochem. Biophys. **54**, 11 (2009).
[3] S. M. Block, C. L. Asbury, J. W. Shaevitz, and M. J. Lang, Proc. Natl. Acad. Sci. U.S.A. **100**, 2351 (2003).
[4] M. J. Schnitzer and S. M. Block, Nature (London) **388**, 386 (1997).
[5] K. S. Thorn, J. A. Ubersax, and R. D. Vale, J. Cell Biol. **151**, 1093 (2000).
[6] S. J. Green, J. Bath, and A. J. Turberfield, Phys. Rev. Lett. **101**, 238101 (2008).
[7] T. Omabegho, R. Sha, and N. C. Seeman, Science **324**, 67 (2009).
[8] R. Pei, S. K. Taylor, D. Stefanovic, S. Rudchenko, T. E. Mitchell, and M. N. Stojanovic, J. Am. Chem. Soc. **128**, 12693 (2006).
[9] P. Yin, H. M. T. Choi, C. R. Calvert, and N. A. Pierce, Nature (London) **451**, 318 (2008).
[10] F. C. Simmel, ChemPhysChem **10**, 2593 (2009).
[11] T. Antal, P. L. Krapivsky, and K. Mallick, J. Stat. Mech.: Theory Exp. **2007**, P08027 (2007).
[12] T. Antal and P. L. Krapivsky, Phys. Rev. E **76**, 021121 (2007).
[13] M. Bonaccio, A. Credali, and A. Peracchi, Nucleic Acids Res. **32**, 916 (2004).
[14] T. K. Stage-Zimmermann and O. C. Uhlenbeck, RNA **4**, 875 (1998).
[15] D. T. Gillespie, J. Phys. Chem. **81**, 2340 (1977).
[16] S. Uemura, K. Kawaguchi, J. Yajima, M. Edamatsu, Y. Y. Toyoshima, and S. i. Ishiwata, Proc. Natl. Acad. Sci. U.S.A. **99**, 5977 (2002).
[17] S. Uemura and S. Ishiwata, Nat. Struct. Biol. **10**, 308 (2003).
[18] S. Liepelt and R. Lipowsky, Phys. Rev. E **79**, 011917 (2009).
[19] K. Svoboda, P. P. Mitra, and S. M. Block, Proc. Natl. Acad. Sci. U.S.A. **91**, 11782 (1994).
[20] N. Thomas, Y. Imafuku, and K. Tawada, Proc. R. Soc. London, Ser. B **268**, 2113 (2001).
[21] J. W. Shaevitz, S. M. Block, and M. J. Schnitzer, Biophys. J. **89**, 2277 (2005).
[22] I. Mills, T. Cvitas, K. Homan, and K. Kuchitsu, *Quantities, Units and Symbols in Physical Chemistry* (Blackwell, Oxford, 1993).
[23] P. Lançon, G. Batrouni, L. Lobry, and N. Ostrowsky, Physica A **304**, 65 (2002).
[24] A. W. C. Lau and T. C. Lubensky, Phys. Rev. E **76**, 011123 (2007).
[25] A. B. Kolomeisky and H. Phillips, J. Phys.: Condens. Matter **17**, S3887 (2005).
[26] J. Beeg, S. Klumpp, R. Dimova, R. S. Gracià, E. Unger, and R. Lipowsky, Biophys. J. **94**, 532 (2008).
[27] S. Saffarian, I. E. Collier, B. L. Marmer, E. L. Elson, and G. Goldberg, Science **306**, 108 (2004).
[28] S. Saffarian, H. Qian, I. Collier, E. Elson, and G. Goldberg, Phys. Rev. E **73**, 041909 (2006).
[29] A. Y. Morozov, E. Pronina, A. B. Kolomeisky, and M. N. Artyomov, Phys. Rev. E **75**, 031910 (2007).
[30] J. Qian, P. Xie, S. X. Dou, and P. Y. Wang, J. Theor. Biol. **243**, 322 (2006).
[31] E. Toprak, A. Yildiz, M. T. Hoffman, S. S. Rosenfeld, and P. R. Selvin, Proc. Natl. Acad. Sci. U.S.A. **106**, 12717 (2009).
[32] J. C. Cochran and F. J. Kull, Cell **134**, 918 (2008).
[33] S. M. Block, Biophys. J. **92**, 2986 (2007).